

A Quantum Theory of the Glass Transition Suggests Universality Amongst Glass Formers

Nicholas B. Weingartner,^{1,2} Chris Pueblo,^{1,2} K. F. Kelton,^{1,2} and Zohar Nussinov^{1,2,3}

¹*Institute of Material Science and Engineering, Washington University, St. Louis, MO 63130, U.S.A.*

²*Department of Physics, Washington University, St. Louis, MO 63130, U.S.A.**

³*Department of Condensed Matter Physics, Weizmann Institute of Science, Rehovot 76100, Israel[†]*

(Dated: March 22, 2022)

Despite decades of intense study, the underlying mechanism of the extraordinary dynamics of liquids approaching the glass transition remains, at best, mischaracterized, and at worst, misunderstood. With sufficiently rapid cooling, any liquid can, in principle, be made to form a glass, displaying an immense increase in viscosity upon supercooling. A principle goal of the glass scientist, then, is to understand the incredible increase in viscosity and determine whether a universal nature underlies the glass transition for all classes of liquids. To this end, numerous theories have been proposed that reproduce, to varying degrees of success, the behavior of the viscosity with temperature. Many of these theories are based around the much celebrated Vogel-Fulcher-Tammann form for the viscosity. Despite the successes of this functional form for various supercooled liquids, it is phenomenological in nature, its prediction of a low temperature thermodynamic singularity has been called into question by numerous experimental investigations. In light of these shortcomings, a new theory of the glass transition has recently been proposed which starts from first principles, using elementary quantum mechanical arguments to derive a form for the viscosity which contains only a single fitting parameter in its simplest form. In this Letter, we critically examine this theory and show that the functional form proposed fits the viscosity data of a diverse group of liquids exceptionally well over a wide temperature range. Furthermore, as predicted by the theory, we find that with the aid of a small dimensionless constant that varies in size from $\sim 0.05 - 0.12$, a universal collapse, *of over 16 decades*, of the viscosity data as a function of temperature. The discovered collapse appears in all known glass-formers spanning silicates, metallic alloy, and organic systems.

PACS numbers: 75.10.Jm, 75.10.Kt, 75.40.-s, 75.40.Gb

Introduction. The glass transition remains one of most intensely studied and debated phenomena in physics and materials science today. Uncovering the underlying mechanism of glassy behavior would represent not only a fundamental advance in modern physics, but also would facilitate the ability to better employ the glass-formation process. This would inevitably lead to the more efficient processing of existing glasses. By comparison to their crystalline counterparts, glasses enjoy substantial advantages, e.g., [1–3]. These have lead to numerous applications in fields as diverse as pharmaceuticals, semiconductors, biomaterials, optical recording, and many others [3–6]. Better understanding may enable the creation of new amorphous materials with far-reaching consequences. A material in its liquid phase is distinguished from a solid by an irregular, non-ordered molecular arrangement, and an associated ability to make large-scale molecular rearrangements in response to fluctuations and perturbations. These rearrangements, known as flow, allow a liquid to relax imposed stresses. A fundamental quantity describing the dynamics of liquids is the viscosity (η), a measure of a liquid’s resistance to flow, and a proxy for the relaxation time of the liquid.

During slow cooling at temperatures sufficiently above melting, T_{melt} , (or, more precisely, the “liquidus temperature” T_l) the liquid viscosity shows continuous, moderate increase with decreasing temperature, which can be well described by an Arrhenius form,

$$\eta = \eta_0 e^{\frac{G}{k_B T}}, \quad (1)$$

where G is a temperature-independent free energy barrier to molecular rearrangement. When the temperature is lowered to T_{melt} , the liquid reaches the limit of stability, its free energy crossing that of a solid phase. Here the liquid gives off a characteristic latent heat and a phase transition occurs. The liquid transforms into a crystal, acquiring long-range structural order and losing its ability to flow; the viscosity of a perfect crystal is infinite.

Because a nucleation to the crystalline phase requires some time, a liquid that is cooled sufficiently quickly through T_{melt} , may bypass crystallization and be ‘supercooled’ to a state of metastable equilibrium at temperatures beneath the melting point. As the temperature of the supercooled liquid drops, its viscosity begins to increase dramatically, by as much as 16 decades over a temperature interval as small as a few hundred Kelvin (this is fantastically demonstrated by the behavior of terphenyl). Eventually, a “glass transition” temperature (T_g) is reached where the viscosity is so large that molecular rearrangements cease on physically meaningful timescales, and the supercooled liquid is deemed a glass. The glass transition, despite its name, is not a thermodynamic transition, it merely reflects the point at which the timescale of atomic rearrangement (relaxation time) exceeds the relevant experimental timescale. Whereas the divergent viscosity and structural arrest of a perfect crystal is due to the appearance of new forces caused by symmetry breaking (long-range order) at the freezing transition, the origin of the rigidity of glasses remains elusive. Supercooled liquids and glasses lack long-range order, instead possessing amorphous particle arrangement. If the rapid rise of the viscosity beneath T_{melt} were simply described by the same Arrhenius form as in Eq. (1), then the glass transition would not be so mysterious. Decreasing the tem-

* weingartner.n.b@wustl.edu

† zohar@wuphys.wustl.edu

perature would remove more and more kinetic energy from the molecules leading to ever increasing scarcity in barrier-crossing molecular rearrangements, giving the appearance of rigidity on realizable timescales. This simple behavior is not the case, however. All glass formers depart from the well-understood form of Eq. (1). The celebrated Vogel-Fulcher-Tamman (VFT) form [7–9],

$$\eta = \eta_0 e^{\frac{B}{T-T_0}}, \quad (2)$$

provides a decent fit to the viscosity of most supercooled liquids over a moderate range of temperatures. In fact, the VFT has become the standard fitting form of the viscosity. As seen in Eq. (2), the VFT form contains three material-dependent fitting parameters, the prefactor η_0 , B , and the temperature T_0 . Despite its apparent successes, two fundamental points must be made about the VFT form. First, it is a purely empirical function, it is not derived from first principles, or any specific theories of glass formation (although it can be reproduced by various theories, see [10–16]). Secondly, it predicts a dynamic singularity at the temperature T_0 which exists beneath the glass transition. This temperature has been shown to be in rough agreement with the Kauzmann temperature associated with vanishing of configuration entropy [17], leading some to postulate that there exists a true equilibrium thermodynamic phase transition in the limit of infinitely slow cooling to T_0 . While the notion that the slow dynamics near T_g is associated with the “ghost” of an underlying phase transition is compelling, experimental evidence suggesting an “ideal glass transition” remains elusive.

Complicating matters further is the fact that different glass forming liquids display a widely varying degree of super-Arrhenius behavior (i.e., an increase of the viscosity as T is lowered that is far more dramatic than that predicted by Eq. (1)). Some supercooled liquids are approximately Arrhenius, whereas others show drastic departure from the Arrhenius form. There exists a broad array of liquids having behaviors in between these extremes. Over twenty years ago, C.A. Angell devised a parameter, called the “fragility” [11], that quantifies the degree of departure from Arrhenius behavior, as well as a classification scheme for the spectrum of behaviors. In a nutshell, Arrhenius liquids are deemed strong (i.e., possess a low fragility value) whereas liquids with large departures are deemed fragile (high fragility value). It is widely accepted that fragility is a significant parameter characterizing the glass transition, and it is believed that fragility may correlate with both structural and dynamic phenomenon. Therefore, any reasonable theory of glass formation and supercooling, must, at the very least, contain a connection with fragility.

Explaining the super-Arrhenius increase of the shear viscosity of supercooled liquids is the primary goal of researchers working in glass science. To that end, numerous theories have been proposed that aim to reproduce the behavior of the viscosity upon cooling, and to provide a physical framework that explains the rich phenomenology associated with the glass transition [10–15, 17, 18]. Many such theories have been proposed and tested, all to varying degrees of success [10–16, 18–26]. In many cases, the functional forms derived for the viscosity are not universal; forms that work well for strong

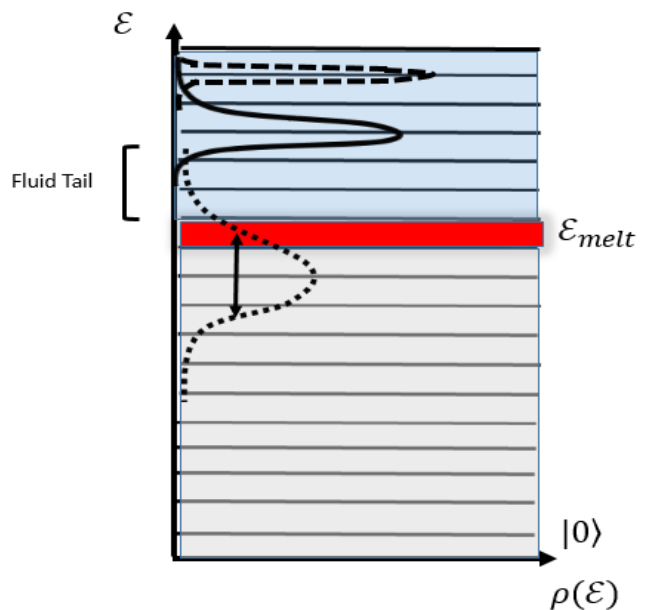


FIG. 1. (Color Online) Simple graphical representation of the DEH. The hierarchy of eigenenergies, \mathcal{E} and their associated eigenstates, with the probability density $\rho(\mathcal{E})$ shown for the high temperature equilibrium liquid (narrow dashed curve), a high temperature non-equilibrium liquid (solid curve), and a supercooled liquid state (dotted curve). For the dotted curve, note that the tail in the fluid-like states is what determines the relaxation time (viscosity).

glasses may not work well for fragile ones, and vice versa. A complete theory of the glass transition, then, should not only provide a fundamental physical explanation of glassy dynamics but also reproduce the behavior of the thermodynamic and kinetic properties of all classes of liquids. Recently, a new theory of the glass transition [27], the ‘Distributed Eigenstate Hypothesis’ (DEH), has been proposed which claims to solve the aforementioned issues. In what follows, we briefly review the basics of the DEH, ultimately arriving at the proposed functional form of the viscosity, which contains only a *single* fitting parameter. We fit this form to a diverse range of glass forming liquids and demonstrate, both qualitatively and quantitatively, that it provides an exceptional fit to the data for many glass formers. We also demonstrate that the notion of fragility appears quite naturally within this framework, and may in fact be intimately linked with glass formability. Finally, as implied by the DEH, we demonstrate that by scaling the data appropriately with the addition of a small single dimensionless parameter, the viscosity of all glassformers studied can be placed on a universal curve that spans 16 decades. This collapse hints at a common underlying mechanism of glass formation in all liquids.

The Distributed Eigenstate Hypothesis. Within the framework of quantum mechanics, the dynamics and evolution of a general N -body system is governed by an appropriately quantized Hamiltonian, \mathcal{H} . For ‘ordinary’ glass forming atomic/molecular liquids (i.e., systems not requiring ad hoc, ‘quenched disorder’ [18]) behaving non-relativistically, the

correct many body Hamiltonian consists of the kinetic energies of all N particles, as well as the complete set of electrostatic interactions between nuclei and electrons in a volume V . Quite generally, then, one can write down the *exact* Hamiltonian of a general N -atom system. The eigenstates and corresponding thermodynamic observables can be obtained by solving the Schrodinger equation,

$$\mathcal{H}|\phi_n\rangle = \mathcal{E}_n|\phi_n\rangle. \quad (3)$$

For macroscopic systems, \mathcal{H} contains many particles. While methods for obtaining approximate solutions exist, in general, the exact eigenstates and associated energies cannot be determined. In spite of this apparent complication, the mere existence of the eigenstates of Eq. (3) (guaranteed by the postulates of quantum theory) allows us to make powerful statements about the dynamical and thermodynamic properties of the system.

We briefly review notions of [27] relevant to our analysis. Long known empirical observations regarding the change of state with temperature and the use of the micro-canonical ensemble for thermal systems, make it clear that high energy eigenstates of \mathcal{H} will correspond to the equilibrium liquid phase, and that low energy eigenstates will correspond to the equilibrium crystalline solid phase. The liquid-like states are separated from the solid-like states by a ‘band’ of eigenstates corresponding to the melting phase transition range (representing the latent heat). The liquid-like eigenstates will be delocalized in the sense that a system within one of these eigenstates can ergodically explore phase space, and will be capable of hydrodynamic flow. Conversely, the solid-like eigenstates will be localized, breaking ergodicity, and possessing the rigidity of the crystalline solid. The symmetry broken solid-like states will necessarily have the long-range structural ordering of the crystalline state built in.

As the premise of any ensemble of statistical mechanics makes clear, when a system (solid or liquid) is in equilibrium, it necessarily includes eigenstates over a narrow energy density interval. Rapidly quenching, by coupling to a heat bath, will drive the system out of equilibrium. The quench will act as a perturbation to the original system, and can be represented by a perturbing Hamiltonian, \mathcal{H}' . The eigenstates of the augmented Hamiltonian, $\mathcal{H}_{Full} = \mathcal{H} + \mathcal{H}'$, will in general *not* be the same as those corresponding to Eq. (3). However, the new state of the system after the supercooling process can, by virtue of the completeness of the eigenstates of \mathcal{H} , be expressed as

$$|\Psi_T\rangle = \sum_n c_n |\phi_n\rangle, \quad (4)$$

where $|\Psi_T\rangle$ is the post-supercooled state corresponding to a temperature, T . As the supercooled liquid is not equilibrium, the effect of the perturbation is to mix the eigenstates of varying energy densities \mathcal{E}_n/V ; this is the defining property of the Distributed Eigenstate Hypothesis (DEH) [27]. The $|c_n|^2$'s that come from projecting $|\Psi_T\rangle$ onto the space $|\phi_n\rangle$ represent the probability distribution of the eigenstates of Eq. (3). A cartoon of this probability distribution $\rho_T(\mathcal{E})$ in the continuum

limit is depicted in Figure (1). As discussed above, the equilibrium state of both the liquid and solid will correspond to a probability density which is δ -peaked at a single eigenstate corresponding to the thermal energy. The mixing brought upon by supercooling, leads to a broadened probability density which encompasses many of the equilibrium eigenstates. In general, the probability density can have weight coming from both the delocalized liquid-like states, and the localized solid-like states. In general, the probability density will shift downward as the temperature is lowered, and the width of the distribution will also change in temperature. In Eq. (4) and Figure 1, only high energy ‘‘liquid like’’ eigenstates (i.e., states $|\phi_n\rangle$ having an energy density \mathcal{E}_n/V exceeding that of the equilibrium system at its melting temperature) contribute to hydrodynamic flow. Recognizing that the relaxation time is proportional the reciprocal of the relaxation rate, and recalling that the relaxation time is proportional to the viscosity, we may express the viscosity in terms of the probability density, namely,

$$\eta(T) \approx \frac{\eta^{eq}(T_{melt})}{\int_{\mathcal{E}_{melt}}^{\infty} \rho_T(\mathcal{E}) d\mathcal{E}} \quad | \quad T \leq T_{melt}. \quad (5)$$

Here, $\eta^{eq}(T_{melt})$ is the value of the equilibrium viscosity at the melting point. The integral in Eq. (5) only includes those states at or above the melting energy. The probability density is ultimately constrained such that $\langle \mathcal{H} \rangle$ is equal to the measured energy E . The simplest form for the probability density that is consistent with this constraint, and is also physically meaningful [27–29] is a Gaussian,

$$\rho_T(\mathcal{E}) = \frac{1}{\sqrt{2\pi\sigma_T^2}} e^{-\frac{(\mathcal{E}-E)^2}{2\sigma_T^2}}. \quad (6)$$

To compute the quintessential form of the viscosity, one may insert Eq. (6) into Eq. (5) and assume that the specific heat does not change significantly. In a more minimal vein, one may consider effective temperatures T_n of the equilibrated system (i.e., eigenstates having an energy $\mathcal{E}_n = U(T_n)$ with U the internal energy of the equilibrated system governed by \mathcal{H}) that are distributed in a Gaussian fashion about the imposed external constraint that the supercooled liquid has a temperature T . Either way, the viscosity of the supercooled liquid is found to be [27]

$$\eta(T) = \frac{\eta(T_{melt})}{\text{erfc}\left(\frac{T_{melt}-T}{2\sigma_T}\right)}. \quad (7)$$

The temperature T is the only natural scale for the width σ_T of the probability density ρ_T formed by general supercooling to that temperature. In light of this and other physical reasoning [27], the simplest form for the width is $\sigma_T = \bar{A} T$ with a dimensionless \bar{A} . Given empirical data, Eq. (7) may be inverted to find the effective σ_T . In the SI, it will be demonstrated that this approximation is very reasonable for most glass formers considered. Putting all of the pieces together, the argument of the complementary error function in Eq. (5) becomes $\frac{T_{melt}-T}{\sqrt{2}\bar{A}T}$,

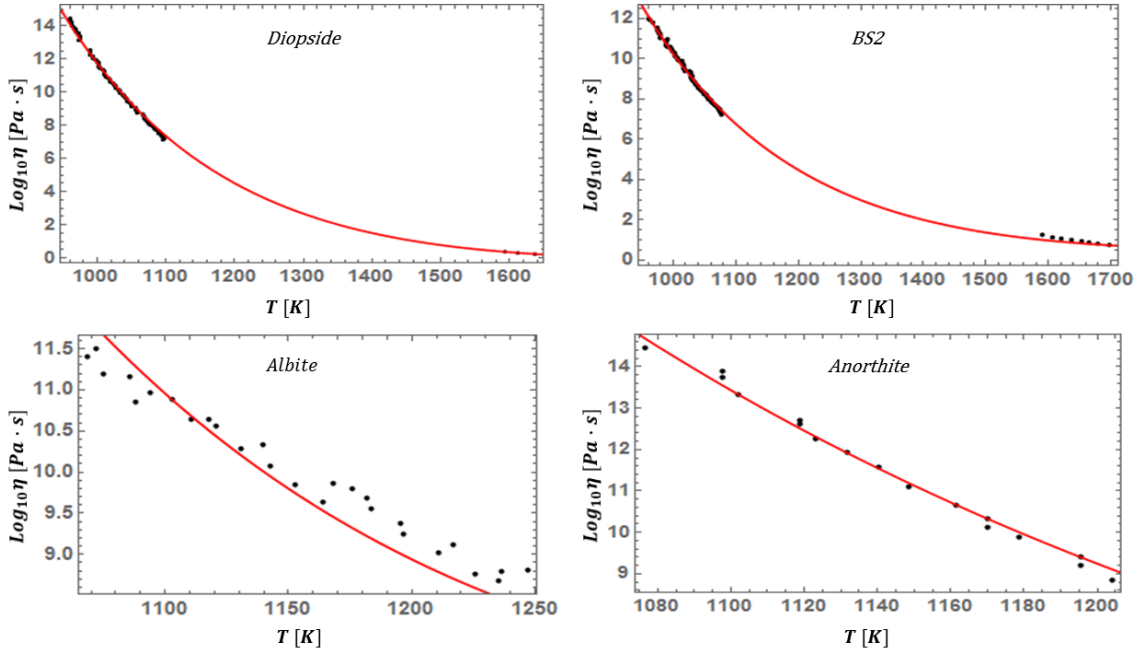


FIG. 2. (Color Online) Fits of the DEH form for the viscosity, Eq. (7), to four silicate glassforming liquids.

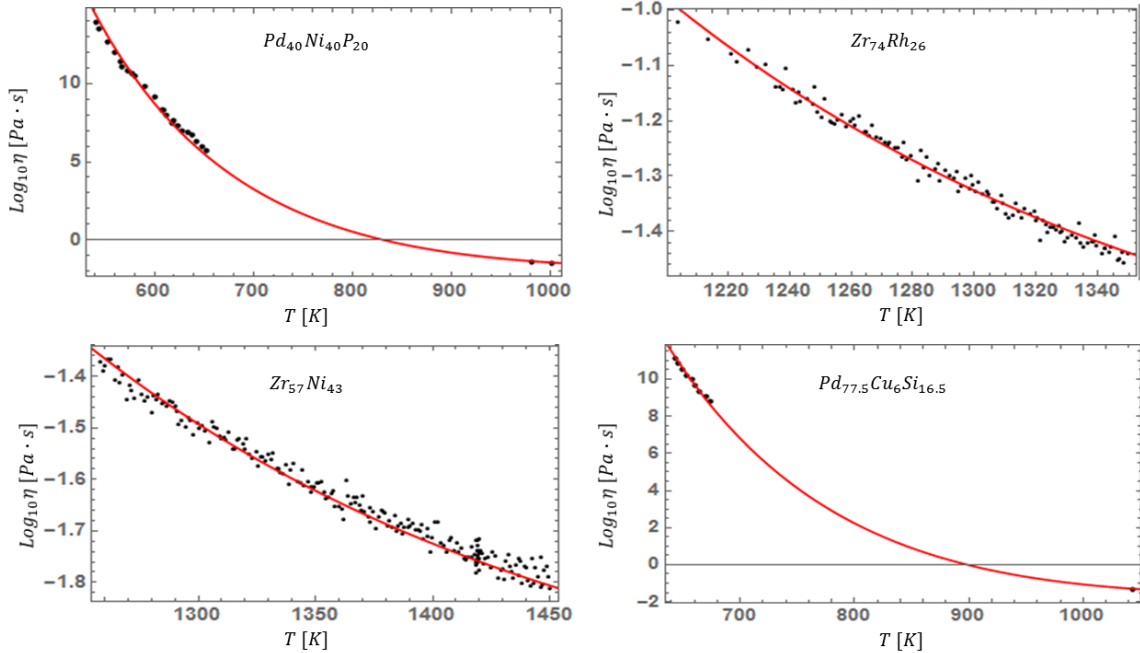


FIG. 3. (Color Online) Fits of the DEH form for the viscosity, Eq. (7), to four metallic glassforming liquids.

with \bar{A} the single parameter of the DEH model. Known melting temperatures of the equilibrated system are listed in the IS (see Table (I) therein).

Application of the DEH Form. To test the validity of the DEH, we examined how well the functional form of Eq. (7) could fit actual experimental viscosity data. We applied the DEH form to the viscosities of eleven different glass forming liquids. As the DEH is meant to be universal across all

types of supercooled liquids, we selected glassformers of all classes, bonding types, and fragilities. We tested five silicate glass formers (Anorthite [30], Diopside, BS2, LS2, Albite [31]), two organics (OTP [32], Salol [33]), and four metallics ($Pd_{40}Ni_{40}P_{20}$, $Pd_{77.5}Cu_6Si_{16.5}$, $Zr_{57}Ni_{43}$, $Zr_{76}Rh_{24}$). The viscosity values of the metallic liquids were extracted from [34] or experimentally measured by us. Data from previous works that was in graphical form was converted to tabular form us-

ing data digitization software. Curve fitting methods were employed to extract the best-fit value of the single parameter, \bar{A} by fitting the DEH form for all temperatures less than or equal to the melting temperature. In some cases, a data point was not present exactly at the melting temperature, requiring minor interpolation of the value of $\eta(T_{melt})$. In all liquids, with the exception of Albite (discussed in the SI), the interpolation was minor, and would, at most, contribute minimal error. In most cases the standard error in the calculation of \bar{A} was of $O(10^{-3})$. In all cases, the fits were applied to the data in natural log form. When plotting the data and corresponding fits, everything was scaled so as to present the data/curves on the more widely used log base 10 form.

Figures (2)-(3) show the logarithm of the viscosity data as a function of temperature with the DEH fits applied. From the figures, it is clear that the DEH form does an exceptional job of fitting the data for the silicate, metallic, and organic glass forming liquids. The only notable exception is the case of Albite which is discussed in the SI. We have demonstrated qualitatively (for quantitative analysis see the SI) that the DEH is capable of very accurately describing the immense dynamical slowdown approaching the glass transition. Furthermore, we have demonstrated its applicability across all classes of supercooled liquids. This is immediately suggestive that the glass transition, in seemingly disparate classes of liquids, has a single, universal, underlying physical mechanism. Eq. (7), involving only a single dimensionless parameter \bar{A} , predicts a collapse of the scaled viscosity $\eta(T)/\eta(T_{melt})$ when plotted as a function of $x \equiv \frac{T_{melt}-T}{T\bar{A}\sqrt{2}}$ [27]. In light of this, we plot in Figure (5), the scaled viscosity of all 11 liquids as a function of the scaled dimensionless temperature x . As seen, the data of the various glass forming liquids is seen to provide an exceptional collapse across 16 decades of viscosities. The gray curve in the figure represents the theoretical curve expected in the DEH. It is reasonable to conclude, then, that the DEH is an excellent candidate for the fundamental theory of glass formation.

Fragility and the crossover temperature. It is widely accepted that the notion of fragility is intimately linked to glassy dynamics, and not just an artifact of “plotting mechanics”. Indeed, recent studies have shown that fragility can be linked to the behavior of the structure factors, and radial distribution functions upon supercooling [35] and therefore represents a measurable physical quantity of significance to glass theory. Therefore, we must briefly examine the nature of fragility in the DEH. Using the definition of the fragility parameter, m , as outlined in [11], the functional form of the fragility can be derived within the DEH framework as

$$m \equiv \left. \frac{d \log_{10} \eta(T)}{d(T_g/T)} \right|_{T=T_g} = \frac{\sqrt{\frac{2}{\pi}} T_{melt}}{\ln(10) T_g \bar{A}} \frac{1}{\operatorname{erfc} \left[\frac{T_{melt}/T_g - 1}{\sqrt{2\bar{A}}} \right]} e^{-\left(\frac{T_{melt}/T_g - 1}{\sqrt{2\bar{A}}} \right)^2}. \quad (8)$$

Strikingly, and perhaps surprisingly, the reduced temperature from the Turnbull criterion [36, 37] for glass forming ability (GFA), $T_{red} \equiv \frac{T_g}{T_{melt}}$, appears throughout this expression. This is suggestive that there is in fact a link between fragility and

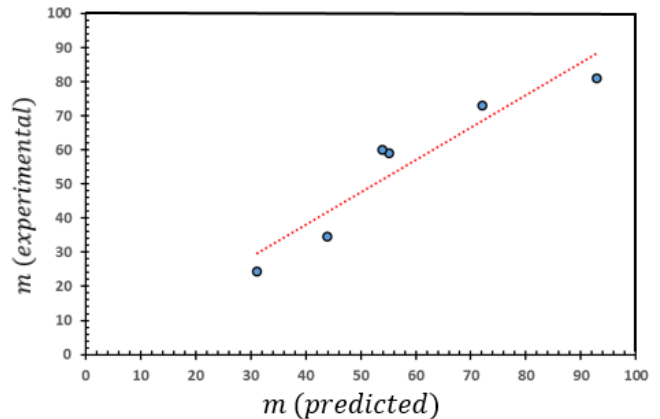


FIG. 4. (Color Online) Experimental values of the fragility, m versus the predicted values using Eq. (8). The slope of the best fit line (dashed-red) is approximately 0.94, which represents very good agreement with experimental values.

GFA. We can calculate the values of the fragility using Eq. (8) and compare with the experimental values reported in [38, 39]. The results of this comparison are depicted in Figure (4) and the values are listed in Table (IV). It is clear from Figure (4) that the DEH expression does a very good job of predicting fragility values. Not only does this provide further support for the theory and the linear approximation, but it also suggests that fragility can be predicted. These ideas will be addressed in more depth in a subsequent paper. A graphical representation of fragility is discussed in the SI.

We briefly remark on another dynamical temperature (T_A) at which point the super-Arrhenius growth of the viscosity sets in, the Stokes-Einstein relation breaks down, phonons delocalize, and cooperative motion first begins [18, 40, 41]. The onset of the above phenomenon has been shown, in molecular dynamics simulations, to be correlated with the onset of structural changes associated with the formation, and subsequent percolation of locally-preferred structures, which may or may not be subunits of the low temperature crystalline order [41, 42]. It seems reasonable, then, that upon cooling, the temperature at which these phenomena begin to occur should correspond to the temperature at which the probability density first has appreciable weight in the solid-like eigenstates. With this in mind, the DEH theory [27] links the parameter \bar{A} and the temperatures T_{melt} and T_A

$$T_A \approx \frac{T_{melt}}{1 - \bar{A}}. \quad (9)$$

The values of T_A that are predicted by Eq. (9) are listed in the SI, and comparisons between prediction and experiment are discussed there. The structural change that has been shown to begin at T_A , as well as the broad phenomenology of this temperature, will be addressed in a subsequent paper. Here, we merely comment that the possible accuracy of Eq. (9), would allow for computing the value of \bar{A} from high temperature liquid data, and hence lead to the DEH being a zero parameter theory.

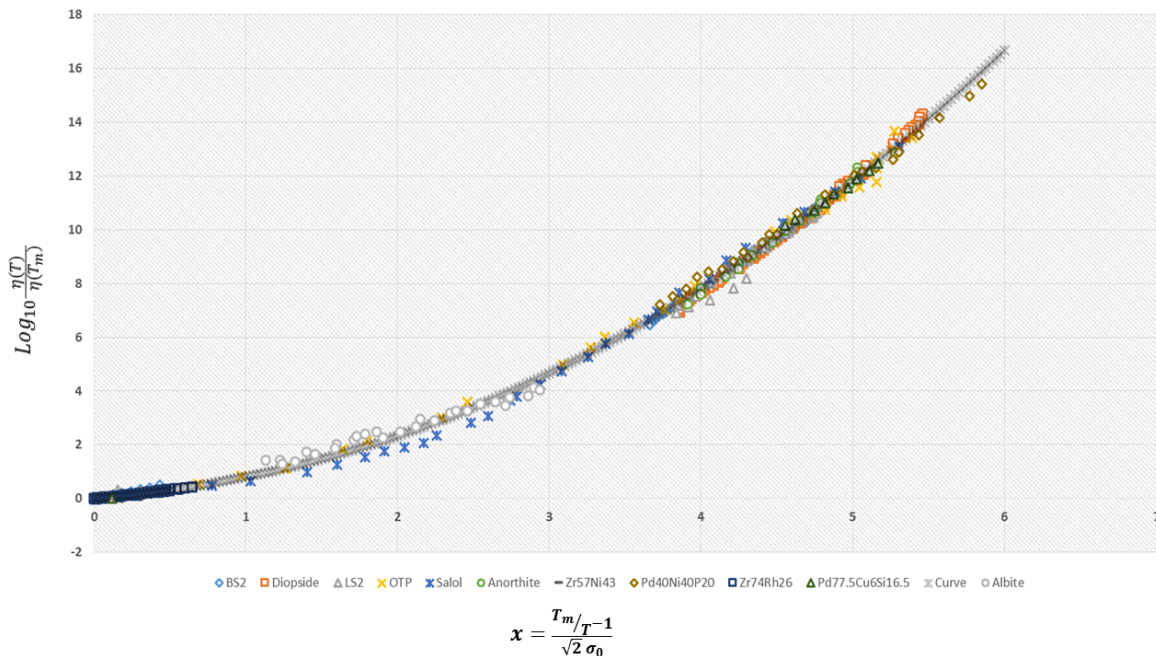


FIG. 5. (Color Online) Viscosity data scaled by its value at the melting point, $\eta(T_{melt})$, versus x , as defined in the figure. The data of all eleven liquids studied, from all classes/bonding types (silicate, metallic, organic) and kinetic fragilities is seen to collapse onto a universal curve. Note the exceptional agreement over at least 7 decades at low temperatures.

Conclusion and Outlook. In this work, we have demonstrated that the DEH can accurately describe the dynamical behavior of supercooled liquids by fitting the functional form predicted for the viscosity to experimental data for all types of glass forming liquids. A statistical analysis revealed exceptional goodness of fit measures for the DEH form, and it was shown that this form could perform better than previous models that possess more fitting parameters. Within the framework of the DEH we were able to make predictions about

fragility and a dynamical crossover temperature, which are shown to be very accurate, adding further validity to the DEH. Beyond checking the prediction of this theory, our found universal collapse of the viscosity over 16 decades with the use of only a single small dimensionless parameter \bar{A} illustrates a quintessential feature of all glass forming liquids found in nature.

Acknowledgements. NW and ZN were supported by the NSF DMR-1411229. ZN thanks the Feinberg foundation visiting faculty program at Weizmann Institute.

-
- [1] L. Berthier and M. D. Ediger, arXiv:1512.03540 (2015); Physics Today, Jan. 2016, to appear
- [2] R. Zallen, "The Physics of Amorphous Solids", John Wiley & Sons, Inc., pages 23-32 (1983).
- [3] A. L. Greer and E. Ma, MRS Bulletin **32**, 611 (2007).
- [4] B. C. Hancock and M. Parks, Pharmaceutical Research **17**, 397 (2000).
- [5] M. Telford, Materials Today **7**, 36 (2004).
- [6] M. Wuttig, and N. Yamada, Nature Materials **6**, 824 (2007).
- [7] H. Vogel, Z. Phys. **22**, 645 (1921)
- [8] G. S. Fulcher, J. Am. Ceram. Soc. **8**, 339 (1925)
- [9] G. Tamann and W. Z. Hesse, Anorg. Allgem. Chem. **156**, 245 (1926)
- [10] L. Berthier and F. Biroli, Reviews of Modern Physics, **83**, April-June (2011) [review]
- [11] C. A. Angell, Journ. Phys. and Chem. of Solids, **49**, 863-871 (1988)
- [12] I. Procaccia, Eur. Phys. J. Special Topics, **178**, 81-122 (2009) [review]
- [13] I. M. Kalogeras and HE. Hagg Lobland, Journal of Materials Education, **34**(3-4): 69-94 (2012) [review]
- [14] G. L. Hunter and E. R. Weeks, Rep. Prog. Phys. **75**, 066501, (2011) [review]
- [15] J. S. Langer, Rep. Prog. Phys., **77**,042501 (2014) [review]
- [16] G. Adam, and J. H. Gibbs, J. Chem. Phys., **43**, 139-146, (1965)
- [17] W. Kauzmann, Chem. Rev., 1948, **43** (2), pp219-256
- [18] A. Cavagna, Physics Reports, **476**, 551-124 (2009) [review]
- [19] T. R. Kirkpatrick, D. Thirumalai, and P. G. Wolynes, Phys. Rev. A, **40**, 1045 (1989)
- [20] T. R. Kirkpatrick and D. Thirumalai, Phys. Rev. Lett., **58**, 2091 (1987)
- [21] T. R. Kirkpatrick and D. Thirumalai, Phys. Rev. B, **36**, 5388 (1987)
- [22] T. R. Kirkpatrick and P. G. Wolynes, Phys. Rev. B., **36**, 8552 (1987)
- [23] T. R. Kirkpatrick and D. Thirumalai, Phys. Rev. B., **37**, 5342 (1988)
- [24] T. R. Kirkpatrick and D. Thirumalai, J. Phys. A, **22**, L149

- (1989)
- [25] D. R. Reichman, and P. Charbonneau, *J. Stat. Mech: Theory and Experiment*, **5**, 05013 (2005)
 - [26] F. Ritort and P. Sollich, *Adv. Phys.*, **52**, 219-342 (2003)
 - [27] Z. Nussinov, “A one parameter fit for glassy dynamics as a quantum corollary of the liquid to solid transition”, arXiv: 1510.03875 (2015)
 - [28] G. E. H. Hentschel, S. Karmakar, I. Procaccia, and J. Zylberg, arXiv: 1202.1127 (2012)
 - [29] M. D. Ediger and P. Harrowell, *J. Chem. Phys.* **137**, 080901 (2012)
 - [30]
 - [31] D. Cranmer and D. R. Uhlmann, *J. Non-Crystalline Solids*, **45**, 283-288 (1981)
 - [32] E. Rossler, and H. Sillescu, “Organic Glasses and Polymers”, *Materials Science and Technology*, ISBN: 3527313958 (2006)
 - [33] F. Mallamace, C. Branca, C. Corsaro, N. Leone, J. Spooren, S. Chen, and H. E. Stanley, *PNAS*, **107(52)**: 2245722462 (2010)
 - [34] K. H. Tsang, S. K. Lee, H. and W. Kui, *J. App. Phys.*, **70**, 4837-4841 (1991)
 - [35] N. A. Mauro, M. Blodgett, M. L. Johnson, A. J. Vogt, and K. F. Kelton *Nature Communications* **5**, 4616 (2014)
 - [36] D. Turnbull, “Under what conditions can a glass be formed?” *Contemp Phys*, **10**,473488 (1969)
 - [37] D. Turnbull, *J. Chem. Phys.* **18**, 198 (1950).
 - [38] M. Nascimento, and C. Aparicio, *J. Phys. and Chem. of Solids*, **68**, 104-110 (2007)
 - [39] M. Blodgett, T. Egami, Z. Nussinov, and K. F. Kelton, *Nature Scientific Reports*, **5**, 13837 (2015)
 - [40] T. Iwashita, D. M. Nicholson, and T. Egami, *Physical Review Letters*, **110**, 205504 (2013)
 - [41] R. Soklaski, Z. Nussinov, Z. Markow, K. F. Kelton, and L. Yang, *Phys. Rev. B*, **87**, 184203 (2013)
 - [42] N. B. Weingartner, R. F. Soklaski, K. F. Kelton, and Z. Nussinov, arXiv: 1508.02736

Supplementary Information.

Quantitative Analysis of the DEH. In the main text, we examined how well the Distributed Eigenstate Hypothesis (DEH) could fit the viscosity data of various glass forming liquids of all classes. The function of (Eq. (7)) reproduced the viscosity of both fragile and strong supercooled liquids of all interaction types. In what follows we do a basic statistical analysis of the DEH. While we examine the fits for all eleven tested glass forming liquids, we take OTP and LS2 as ‘case studies’. Figure [S1] shows the DEH fit to the log of the viscosity as a function of temperature for OTP and LS2. We immediately see, that by any objective visual measure, the single parameter fits are exceptional.

As a first step to more rigorously assessing the quality of the fits, we examine the residuals of the fits,

$$Res(T) \equiv \sum_i (\eta(T_i) - f(T_i)). \quad (10)$$

Here, $f(T)$ is the temperature dependent function being tested. Figure [S2] displays the results of the residual analysis for a random sample of the glass forming liquids studied. In all cases the magnitude of the residuals is very small, and this is true for LS2 and OTP (with the exception of two outlying points for OTP). The low magnitude of the residuals is immediately suggestive that the DEH form well approximates the actual data. The fit must not only approximate the data, but must also be capable of accounting for the variation in the data. If the DEH is to account for this variation up to the random measurement error of the data, the residuals should be more or less random, without significant biasing. From the plots of the residuals, it is clear that in most cases there is very little biasing. The only notable exception is Salol, which is discussed below, along with a discussion of the cause behind any minor bias that appears in the residuals of Figure [S2].

Continuing to expand our analysis, we next calculate three statistical goodness of fit (GoF) measures of the DEH form to the experimental data. For each composition considered we compute the sum of squared errors (SSE), reduced chi-squared value ($\chi^2_{reduced}$), and r-squared value (R^2), as defined below.

$$SSE \equiv \sum_i (\eta(T_i) - f(T_i))^2 \quad (11)$$

$$\chi^2_{reduced} = \sum_i \frac{(\eta(T_i) - f(T_i))^2}{n_{data} - n_{parameters}} \quad (12)$$

$$R^2 \equiv 1 - \frac{SSE}{SST} = 1 - \frac{\sum_i (\eta(T_i) - f(T_i))^2}{\sum_i (\eta(T_i) - \bar{\eta})^2} \quad (13)$$

The calculated values of the statistical GoF measures are listed in Table (II), in the rows labeled “DEH”. Typically, statistically high quality measures of GoF correspond to a $\chi^2_{reduced}$ value that is less than one, R^2 asymptotically close to one and low SSE. As seen in the table, the lowest value of $\chi^2_{reduced}$ does not necessarily correspond to the highest value of R^2 and vice versa, although overall the values are largely correlated. This makes clear, however, that a rigorous statistical analysis

TABLE I. Relevant Temps

Composition	T_{melt} [K]	T_g
LS2	1307	727
Diopside	1664	995
Anorthite	1825	1113
Salol	315	220
OTP	329.35	240
Albite	1393	1087
BS2	1699	973
$Zr_{57}Ni_{43}$	1450	N/A
$Zr_{74}Rh_{26}$	1350	N/A
$Pd_{40}Ni_{40}P_{20}$	1030	560
$Pd_{77.5}Cu_6Si_{16.5}$	1058	N/A

requires both values together. For our “case study” compositions of OTP and LS2, we see that in both cases, the values of $\chi^2_{reduced}$ are lower than 0.5 and have values of R^2 which are greater than 0.98. In fact, a close examination of the calculated statistical values in Table (II) makes clear, that in all liquids studied, the highest value of $\chi^2_{reduced}$ is 0.55, well below unity. Similarly, the lowest calculated value of R^2 is 0.87. This low value of R^2 corresponds to the case of Albite, which was seen to provide the worst fit in the main text. In the case of Albite, a value of η in the vicinity of T_{melt} (required for Eq. (7)) was not available, but in this case the interpolation was large, as the closest data points were 80-100K away on either side (for more discussion of possible error, see below section). Taken together, the residual and statistical analyses, combined with the considerations discussed in the main text, all objectively lead to the conclusion that the DEH accurately represents the viscosity data. For data sets with multiple measurements, one could even go further, and use a more rigorous $\chi^2_{reduced}$ statistic involving the variance at each temperature, and also include cross-validation techniques. We will not perform this analysis here, but will briefly report that for $Zr_{74}Rh_{26}$, a second data set was available, and that fitting of the DEH form led to a value of \bar{A} that was within 3 percent of the value from the first fit. In fact, fitting the second set, with the value of \bar{A} from first set, still maintained an exceptional fit quality, as seen in Figure [S3]. In making the case that the DEH is the appropriate underlying theory of the glass transition, it is important to not only demonstrate the validity of its predictions, but also to compare them with the predictions of the previously proposed theories. To that end, we compare and contrast the DEH with five of the most widely used functional forms for the viscosity. We selected a glass forming liquid from each of the three classes considered, namely organic (OTP), silicate (LS2), and metallic ($Pd_{77.5}Cu_6Si_{16.5}$) and fit the functional forms (listed below) arising from the KKZNT avoided critical point model [1–3], Cohen-Grest free volume model [4], BENK modified parabolic model [5–7], MYEGA entropy model [8], and the oft-employed VFT form

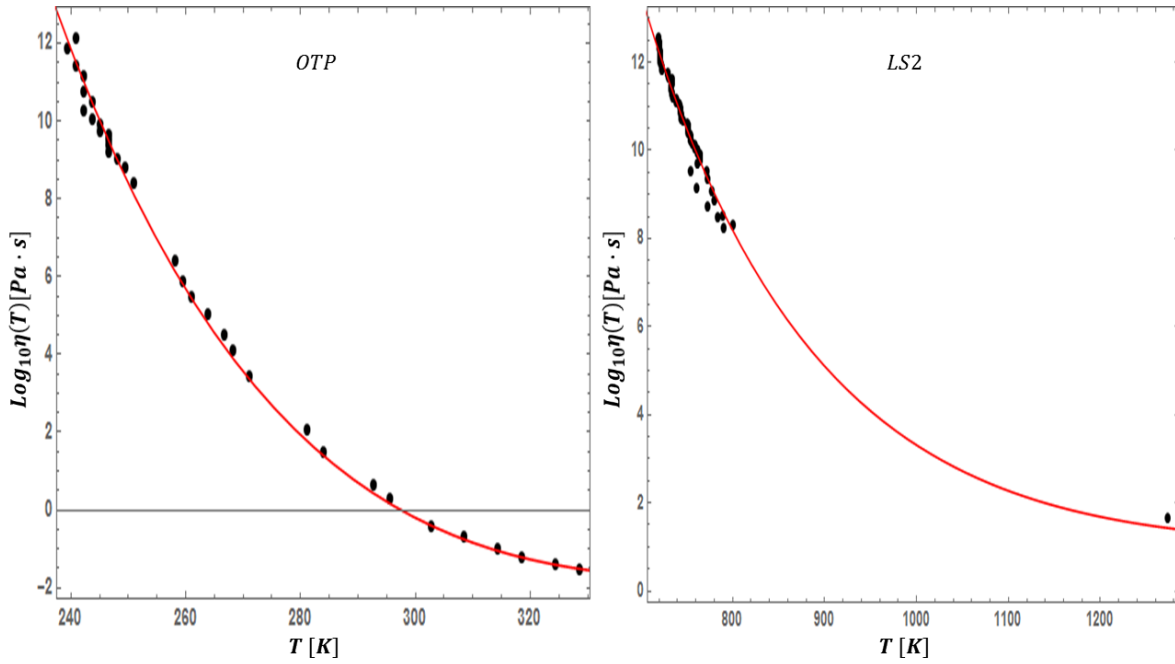


FIG. 6. (Color Online) Data of $\log \eta(T)$ as a function of T for very fragile OTP and very strong LS2 with DEH fits applied. The single parameter fit of Eq. (5) is shown to do an excellent job for both glass formers.

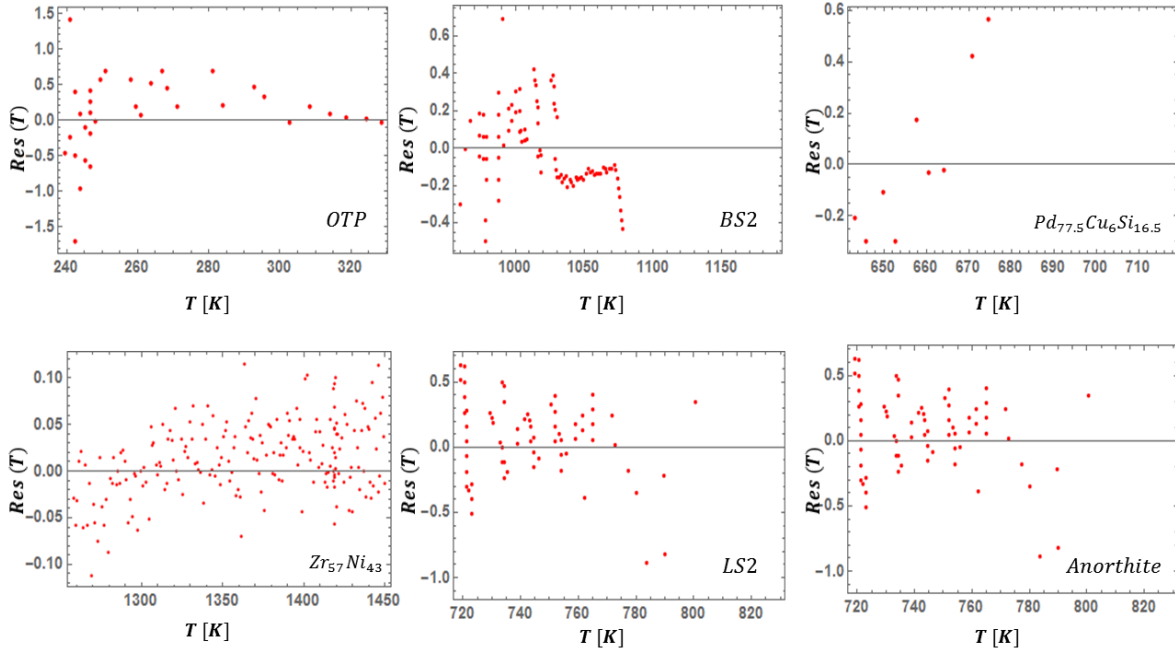


FIG. 7. (Color Online) Plots of the Residuals of the DEH fits to the viscosity data of 6 glassforming liquids studied.

(Eq. 2 in the main text).

$$\ln \eta = \ln \eta_0 + \frac{E_\infty}{T} + \frac{T_A}{T} B \left[\frac{T_A - T}{T_A} \right]^c \Theta(T_A - T) \quad (KKZNT)$$

$$\ln \eta = \ln \eta_0 + \frac{2B}{T - T_0 + \sqrt{(T - T_0)^2 + CT}} \quad (Cohen - Grest)$$

$$\ln \eta = \ln \eta_0 + \frac{E}{k_B T} + J^2 \left(\frac{1}{T} - \frac{1}{\tilde{T}} \right)^2 \Theta(\tilde{T} - T) \quad (BENK)$$

$$\ln \eta = \ln \eta_0 + \frac{K}{T} e^{\frac{c}{T}} \quad (MYEGA)$$

Each of these functional forms (including VFT) has at least three parameters that cannot be determined from first principles. In order to determine the parameters of the various forms for the three test liquids, we fit the natural log of the viscosity data. In all cases, we first fit the high temperature (above melting) $\log \eta$ data as a function of reciprocal temperature, with a straight line. This allows us to extract values of the prefactor,

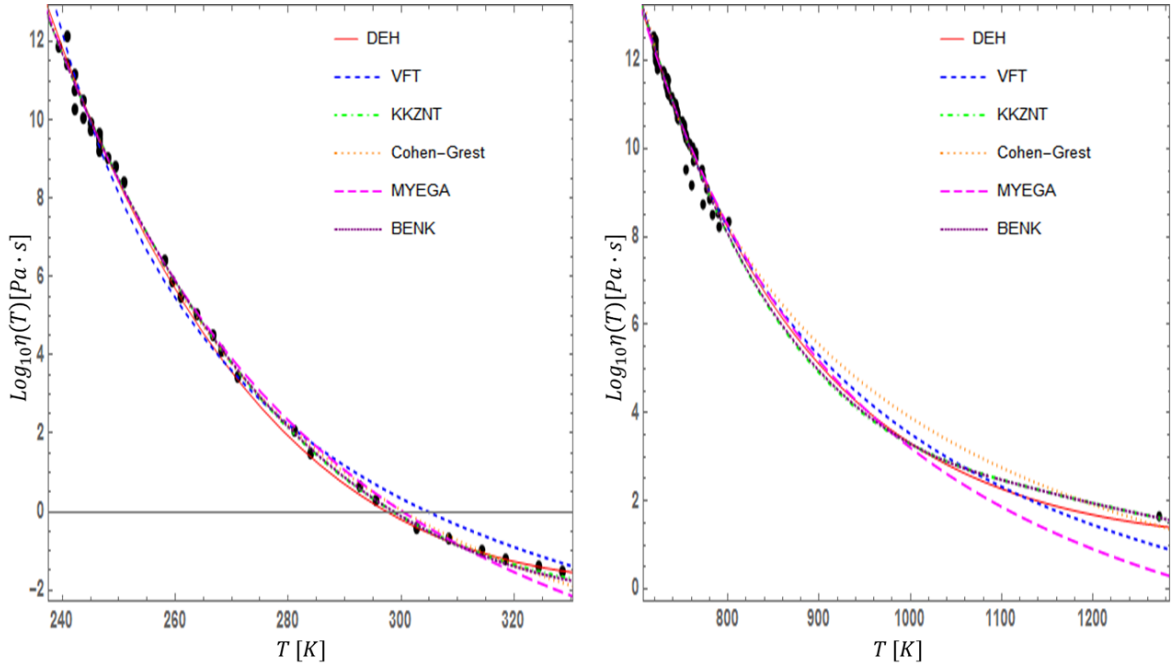


FIG. 8. (Color Online) Comparison of DEH, VFT, KKZNT, Cohen-Grest, MYEGA, and BENK forms for the viscosity as applied to fragile OTP and strong LS2.

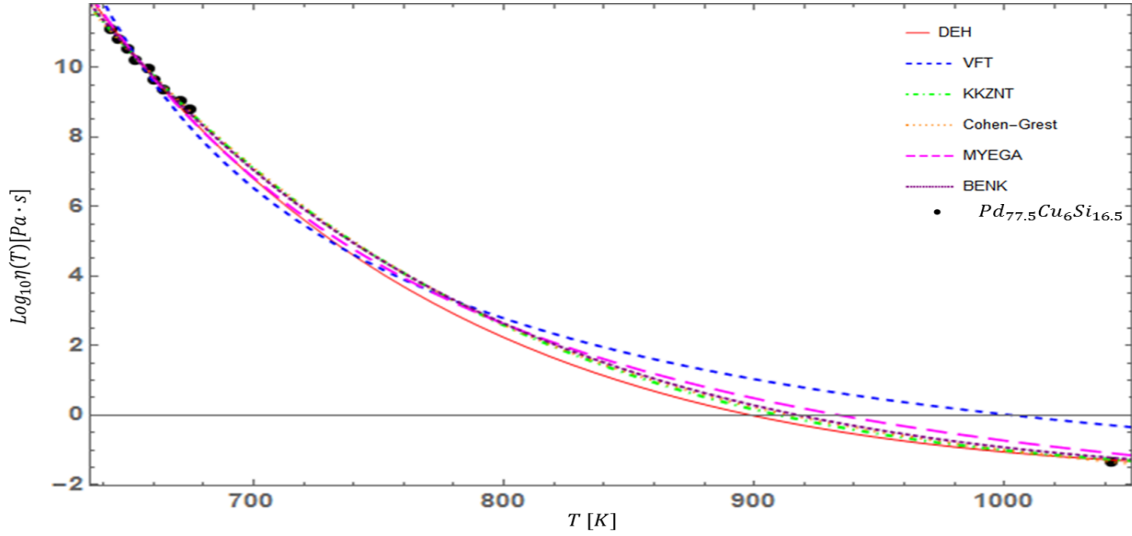


FIG. 9. (Color Online) Comparison of DEH, VFT, KKZNT, Cohen-Grest, MYEGA, and BENK forms for the viscosity as applied to the metallic liquid $Pd_{77.5}Cu_6Si_{16.5}$.

η_0 , and the infinite temperature activation energy, E (or E_∞), where relevant. For each liquid, we fixed these values and then fit the data over the temperature range from T_{melt} and below, to find the values of the remaining parameters. In the case of KKZNT, we also constrained the parameter z to be $\frac{8}{3}$ (see [1] for discussion). After finding values for all the parameters, we examined all of the fits (including DEH) on the same plots as depicted in Figures (S4) and (S5). In Figure (S6) we plot the residuals of all the forms together. Visually it is clear that the VFT form consistently provides the worst fit. The other

forms all appear fairly similar, qualitatively. The residuals are more or less consistent across the forms, with the exception of VFT, which as expected shows significant bias, especially in the case of OTP. We applied the same quantitative statistical analysis to the five additional forms as we did to the DEH fits. The results of this analysis are presented in Table (II) in the rows with the appropriately corresponding headings. The calculations show that the DEH form consistently outperforms the VFT, and MYEGA forms across all classes. The Cohen-Grest form appears to be roughly similar to the DEH form,

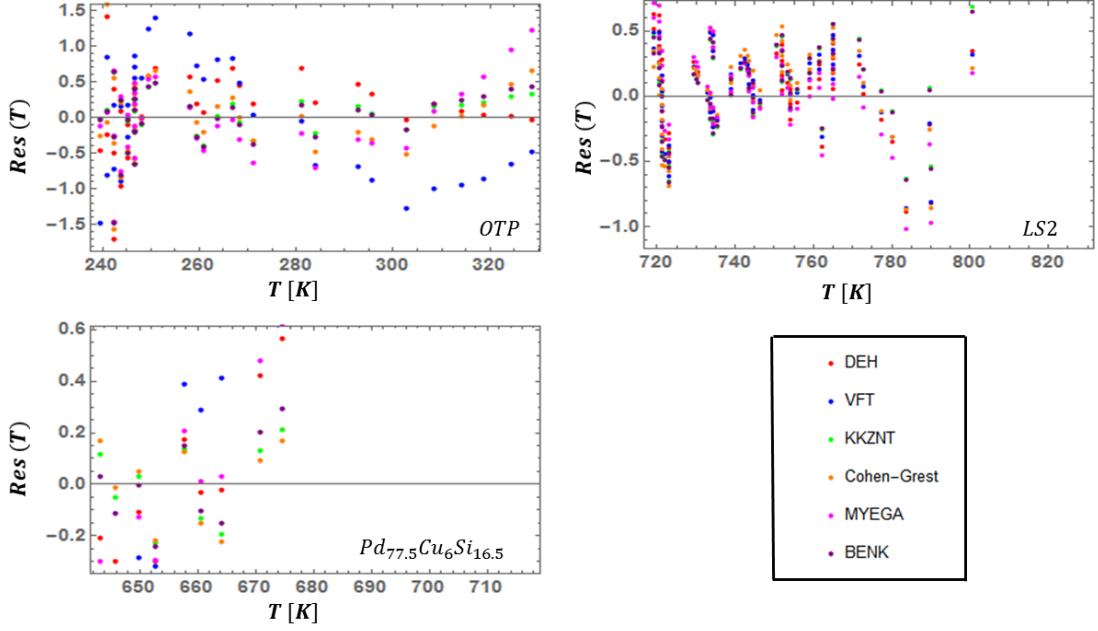


FIG. 10. (Color Online) Comparison of the residuals of the DEH, VFT, KKZNT, Cohen-Grest, MYEGA, and BENK fits to OTP, LS2, and $Pd_{77.5}Cu_6Si_{16.5}$.

TABLE II. Statistical Measures of GoF

Composition	Function	(SSE)	χ^2_{red}	R^2
OTP	DEH	10.617	0.312264	0.997247
	VFT	24.5584	0.767451	0.993632
	KKZNT	8.67516	0.279844	0.997751
	CG	9.66624	0.30207	0.997494
	BENK	8.91119	0.270036	0.997689
	MYEGA	12.3813	0.386916	0.99679
LS2	DEH	14.8497	0.215213	0.983678
	VFT	16.5523	0.247049	0.981807
	KKZNT	13.3202	0.201821	0.985359
	CG	14.8216	0.221218	0.983709
	BENK	13.3526	0.196361	0.985324
	MYEGA	24.9113	0.371811	0.972619
$Pd_{77.5}Cu_6Si_{16.5}$	DEH	0.789078	0.0876754	0.998759
	VFT	10.2834	1.46905	0.983823
	KKZNT	0.235779	0.0392965	0.999629
	CG	0.203843	0.0291204	0.999679
	BENK	0.334157	0.0417696	0.999474
	MYEGA	1.31174	0.187391	0.997937
Salol	DEH	17.1643	0.553687	0.993136
Diopside	DEH	13.1776	0.0941259	0.997362
Anorthite	DEH	2.25807	0.141129	0.991396
BS2	DEH	4.902	0.0505361	0.998646
Albite	DEH	13.3105	0.511942	0.87503
$Zr_{74}Rh_{26}$	DEH	0.115181	0.000984452	0.983959
$Pd_{40}Ni_{40}P_{20}$	DEH	12.3782	0.515757	0.993153
$Zr_{57}Ni_{43}$	DEH	0.351164	0.00172139	0.977947

whereas the KKZNT and BENK forms consistently outperform the DEH. At first glance this would seem to be a concern for the theory, however, Cohen-Grest, KKZNT, and BENK

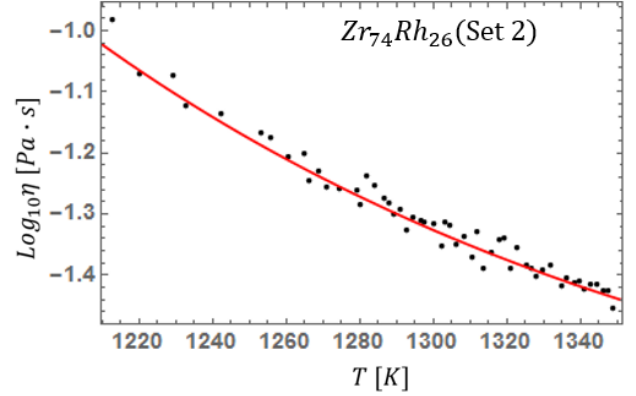


FIG. 11. (Color Online) Examination of the DEH fit for a second set of $Zr_{74}Rh_{26}$ data. The parameter \bar{A} was fit using the first set. It is seen that, although the second set of data predicted a slightly different value for \bar{A} (likely due to simple measurement variance), the fit is still exceptional.

have significantly more parameters. It was also found that in many cases, the values of the “special temperature” parameters providing the exceptional fits/statistics did not correspond to physically reasonable values.

For LS2, both the KKZNT and BENK fits gave parameters for the crossover temperature that were roughly hundreds of kelvin below where it would reasonably be expected to be by simply visually examining the data. When the temperature parameters were fixed to more reasonable values and the remaining parameters then fit, the fit quality of KKZNT and

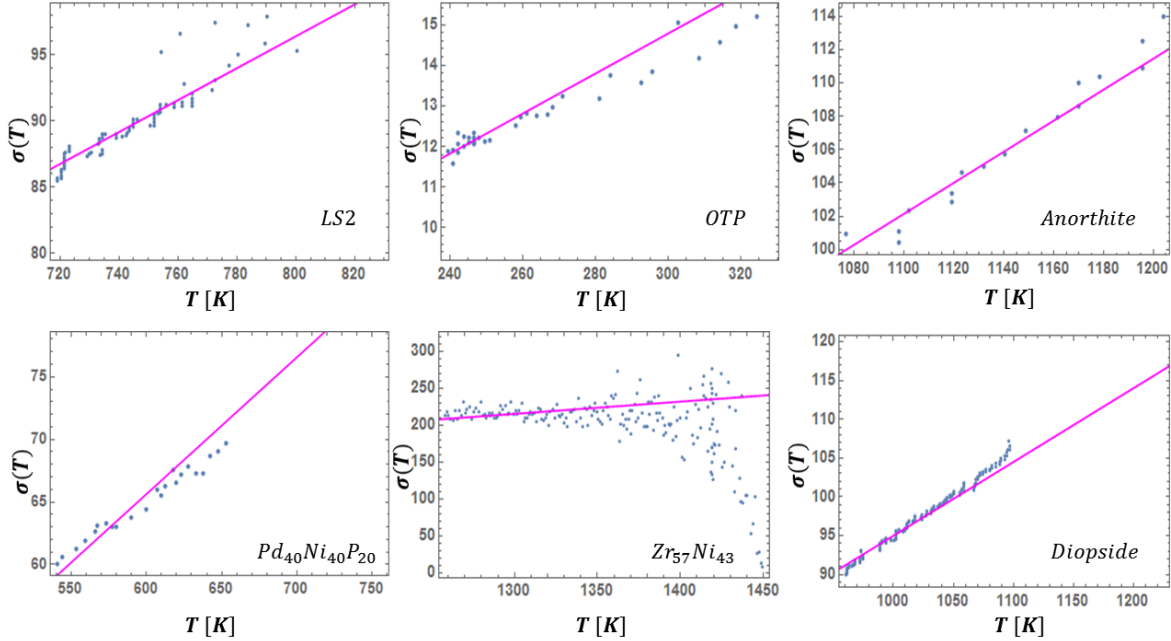


FIG. 12. (Color Online) Plot of σ as a function of T . The fit from the linear approximation (magenta curve) is shown to work very well for most cases.

BENK changed dramatically, providing a very poor fit for LS2. This is consistent with previous results that suggested that the KKZNT form did work for silicate glassformers. It had also been previously reported that the MYEGA form did not accurately reproduce the behavior of metallic glass forming liquids, and we have found that Cohen-Grest performs poorly for the organic OTP. Therefore, one can conclude that the functional forms of previous theories are not universal. In the text, we have shown that the DEH is indeed universal, and coupled with the statistical comparison performed here, can conclude that is an excellent candidate to describe the phenomenology of the glass transition.

Temperature Dependence of $\sigma(T)$. The temperature dependence of $\sigma(T)$ can be solved for by inverting Eq. (5) in the text. Figure (S7) shows the behavior of $\sigma(T)$ for the various glass forming liquids. It is clear that in almost every case, the linear approximation ($\sigma(T) = \bar{A}T$) is incredibly accurate over the temperature range considered. This provides further support for the DEH, and the fragility and T_A predictions discussed in the text. The fit quality could, in general, be further improved by allowing $\sigma(T)$ to have a constant term added to it, such that $\sigma(T) = \sigma_0 T + b$. As the slope itself (our parameter \bar{A}) is generally correct, but the intercept is not exactly zero. As discussed above, however, $\sigma(T)$ must go to zero as the temperature approaches absolute zero, so a nonzero intercept is not reasonable. Therefore, a slight changeover, or curvature may be expected to occur at low temperature. This is addressed in [9] and will be studied in a future work. The most notable outlier to the linear approximation is the case of salol, shown in Figure (S8). Interestingly, it was shown in [33], that Salol may undergo a so-called “fragile-strong” crossover in the range $T_g \leq T \leq T_{melt}$. This may be an elusive liquid-liquid

($l-l$) phase transition, and the exact temperature of its occurrence was suggested to be at $T_{l-l}=256$ K [10]. A system undergoing a phase transition or phase separation would not be expected to be able to be fit by a single form with a single parameter, which could lead to the discrepancy in the Salol fit. The most interesting facet of this possible transition is that in examining the behavior of σ_T in Figure (S8) for Salol, it is clear the the linear approximation breaks down at exactly the same temperature at which the putative liquid-liquid transition occurs, $T \approx 256$ K! Therefore, it may be possible for the DEH form to predict the existence and location of liquid-liquid phase transitions or crossovers, based on a change in the behavior of $\sigma(T)$. The precise physical significance/meaning of this will be addressed in a future work.

Prediction of T_A .

In the text it was briefly mentioned that the dynamical crossover temperature, T_A , from Arrhenius to Super-Arrhenius behavior, could theoretically be predicted within the DEH framework. Using the values of \bar{A} that were found in the fitting and using Eq. (9), we have predicted the values of T_A for the various glass forming liquids studied. The results are listed in Table (III). For OTP, the value is in good agreement with previously reported results [cite], and also in agreement with the KKZNT value (KKZNT was shown to be reasonable for organic liquids). For $Pd_{40}Ni_{40}P_{20}$, we predict a value of $T_A=1157$ K and the experimentally measured value is 1171 K. The viscosity data for Diopside and LS2 are shown in Figure (S9). Visually, T_A is canonically interpreted as roughly the point where the viscosity starts to show curvature. By examining the figure, it is clear that the predicted T_A values of 1839 K and 1486 K, for diopside and LS2, respectively, are very reasonable. The approximation in Eq. (9) is very rough,

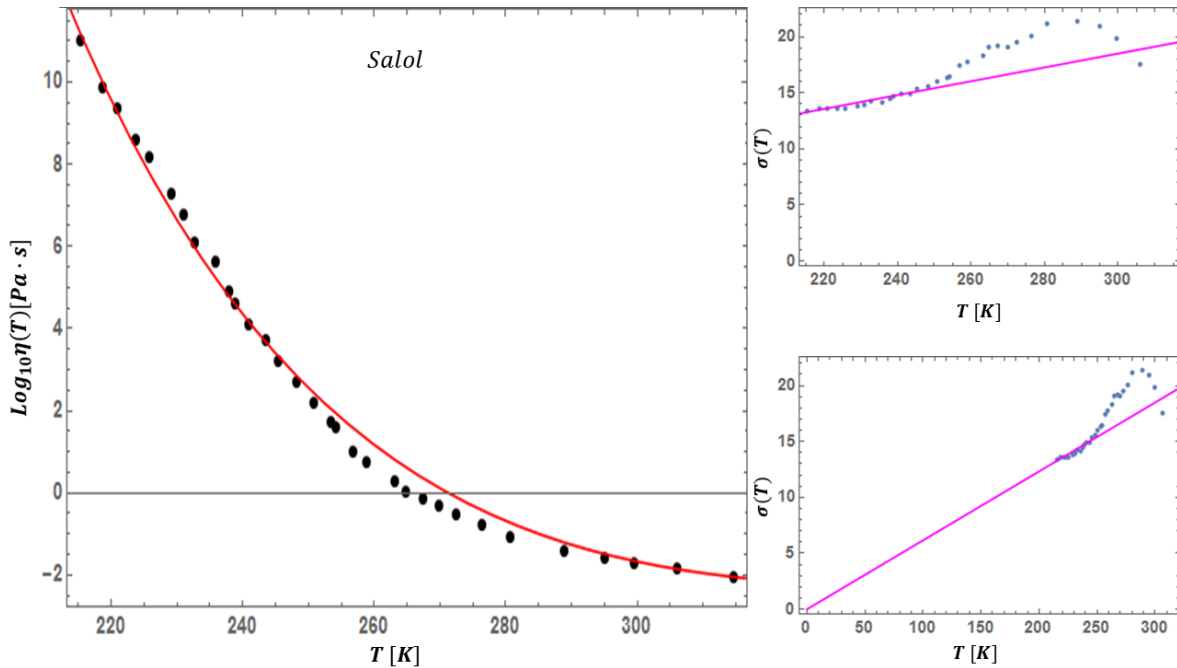


FIG. 13. (Color Online) Left: DEH fit to the viscosity of Salol. The intermediate region of data where the DEH fit appears to “fail” corresponds to the region where the linear approximation breaks down and, in fact, to a temperature where a putative liquid-liquid phase transition was earlier suggested to occur (see text). Right: (Top) The temperature dependence of $\sigma(T)$. The linear approximation fit from Eq. (5) (shown in magenta) works well over a large range of temperatures, but appears to break down upon approach to $T \approx 256\text{K}$ from below. (Bottom) $\sigma(T)$, this time with the range extended to the origin.

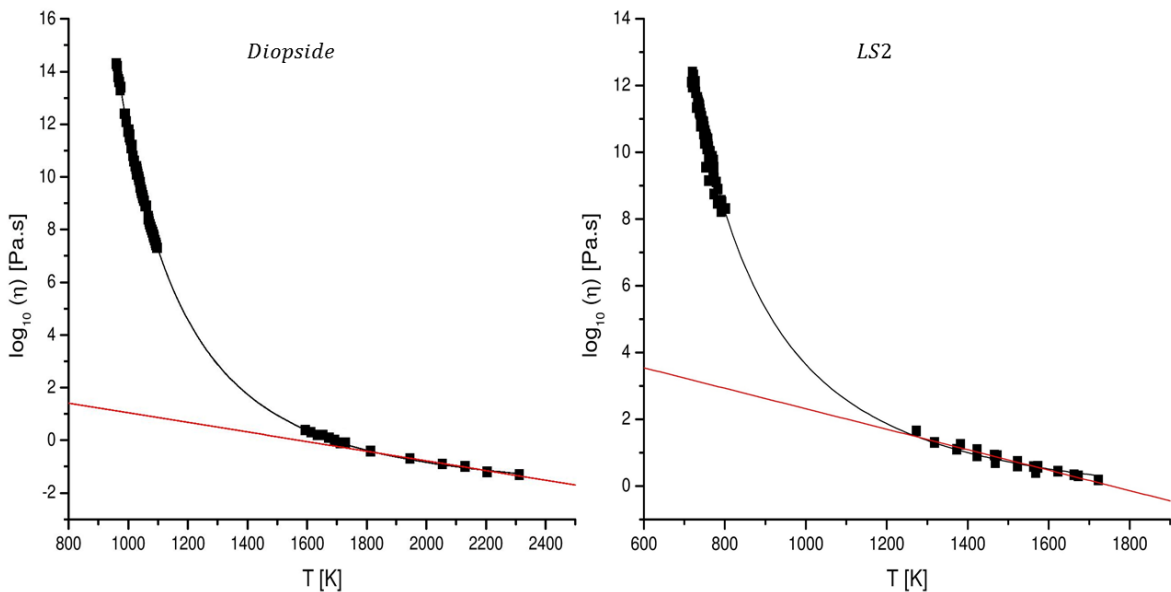


FIG. 14. Viscosity Data as a function of temperature for Diopside and LS2. The changeover from Arrhenius behavior appears to occur in the vicinity of 1900 K for diopside and 1450-1500 K for LS2, roughly agreeing with predicted values for the crossover temperature T_A .

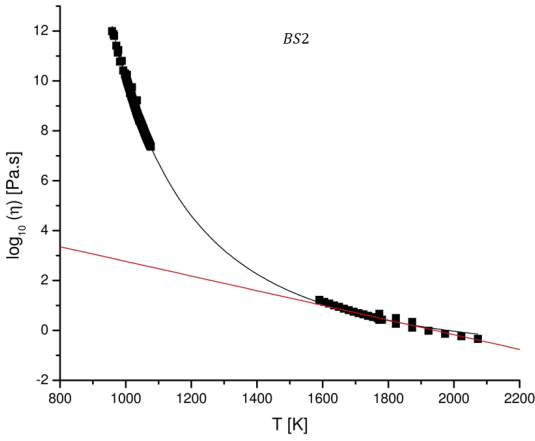


FIG. 15. Viscosity Data as a function of temperature for BS2. The changeover from Arrhenius behavior appears to occur in the vicinity of 1750 K. The predicted crossover temperature T_A was 1911 K. This agrees to within roughly ten percent.

TABLE III. Predicted values of T_A from Eq. (9).

Composition	T_A (Predicted) [K]
Borate	766
LS2	1486
Diopside	1839
Anorthite	2012
Sodium Borate	1102
Salol	336
O-terphenyl	346
LB2	1291
Albite	1503
BS2	1911
Zr ₅₇ Ni ₄₃	1738
Zr ₇₄ Rh ₂₆	1557
Pd ₄₀ Ni ₄₀ P ₂₀	1157
Pd _{77.5} Cu ₆ Si _{16.5}	1160

so some minor error is to be expected. It must be pointed out, however, that the correspondence is not always perfect. For example, we predict a T_A value of 1911 for BS2, and by examining the viscosity data for BS2 in Figure (S10) it is clear that this value is likely to high. In addition, for $Pd_{77.5}Cu_6Si_{16.5}$, we predict a value of $T_A=1160$ K, whereas as experiment suggests $T_A=1313$ K. In these two cases, the predicted and measured values are still within less than ten percent of each other, suggesting very good overall agreement. This is significant, because the relationship between T_A and \bar{A} can work the other way around. Using a measured value of T_A , which is in general a high temperature above T_{melt} and therefore easier to identify than T_g , it would be possible to infer the value of \bar{A} . This would allow us to not only predict the values and behavior of the viscosity of any supercooled liquid below T_{melt} , but by the definition of T_g , the glass transition temperature could also be inferred. This would allow us to use Eq. (8) to predict the fragility of the liquid as well as use the Turnbull criterion to estimate glass forming ability. It was shown in [7] that for all metallic glass forming liquids studied, that the relationship

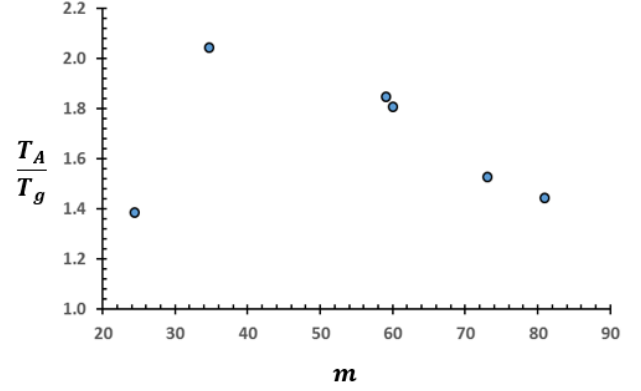


FIG. 16. Ratio of predicted T_A from the the DEH theory to experimentally measured T_g plotted against the measured fragility.

TABLE IV. The values of \bar{A} , predicted fragility, and accepted values of fragility.

Composition	\bar{A}	m (Predicted)	m (Exp)
LS2	0.12048	44	34.7
Diopside	0.094984	55	59.1
Anorthite	0.092875	54	60
Salol	0.061654	72	73
OTP	0.049275	93	81
Albite	0.073075	31	24.4
BS2	0.11107	49	N/A

$T_A \approx 2T_g$ holds. This relationship can allow for testing of this theory.

We can also examine the average ratio of $\frac{T_A(\text{predicted})}{T_g}$ across the other two classes. We found that on average the predicted ratio of T_A to T_g was 1.808 for silicate liquids and 1.485 for organic liquids. The ratio of T_A and T_g is clearly not equal across all classes, and metallics tend to have the highest ratio. We will not further elaborate on this interesting trend here. Beyond the discussion in the main text, it is also interesting to further examine the relationship between the Turnbull temperature ratio [12, 13] and fragility. For the predicted T_A 's, this is shown in Figure (S11). The relationship appears to be non-monotonic, peaking in the middle of the fragility range. This result is interesting, but will not be further addressed here.

A DEH "Angell Plot". Long ago, Angell [14] plotted the viscosity of all known glass formers relative to the dimensionless temperature ratio (T_g/T). The widely varying behavior of the viscosity with temperature led to the introduction of the concept of the fragility. The behavior of the fragility within the DEH form was addressed in the text. There it was shown that the DEH fragility values are in good agreement with those measured in experiment. It was concluded that fragility arises quite naturally within this framework. It is worth briefly pointing out, that by scaling the viscosity by its value at the melting point, $\eta(T_{melt})$, and the reciprocal temperature by the melting temperature, T_{melt} , that a sort of an "Angell Plot" can be generated. This is depicted in Figure (S12). It is clear by looking at the plot, that "bands" of fragility appear in an overall

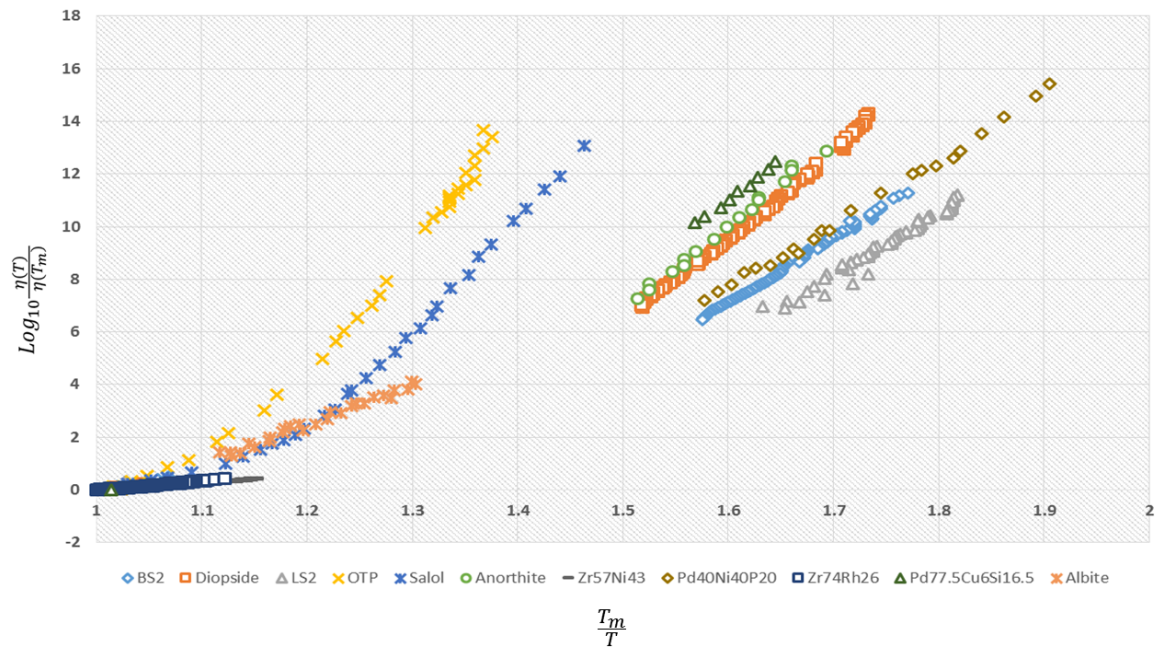


FIG. 17. (Color Online) Natural logarithm of $\eta(T)$ scaled by $\eta(T_l)$ as a function of the scaled temperature, $\frac{T_m}{T}$. When represented this way, a spectrum of behaviors appears, with most glassformers seeming to fall within ‘bands’ corresponding to fragility classes as defined by experimental values.

spectrum of behaviors, ranging from fragile liquids show dramatic increase on the left side of the plot, the growth becoming more gradual as you move “rightward” to higher fragility glass forming liquids. This plot only necessitates having the

melting temperature T_{melt} , and allows one to roughly gauge the relative fragilities of supercooled liquids, without having to measure T_g .

-
- [1] D. Kivelson, S. A. Kivelson, X. Zhao, Z. Nussinov, and G. Tarjus, “A thermodynamic theory of supercooled liquids”, *Physica A*, **219**, 27-38 (1995)
- [2] G. Tarjus, S. A. Kivelson, Z. Nussinov, and P. Viot “The frustration-based approach of supercooled liquids and the glass transition: a review and critical assessment”, *J. Phys: Condens Matter*, **17**, R1143-R1182 (2005)
- [3] Z. Nussinov, “Avoided phase transitions and glassy dynamics in geometrically frustrated systems and non-Abelian theories”, *Phys. Rev. B*, **69**, 014208 (2004)
- [4] M. H. Cohen and G. S. Grest, “Liquid-Glass Transition, a Free-Volume Approach”, *Phys. Rev. B*, **20**, 1077-1098 (1979)
- [5] Y. S. Elmatad, D. Chandler, and J. P. Garrahan, “Corresponding states of structural glass formers”, *J. Phys. Chem. B*, **113**, 5563-5567 (2009)
- [6] Y. S. Elmatad, R. L. Jack, D. Chandler, and J. P. Garrahan, “Finite-temperature critical point of a glass transition”, *PNAS*, **107**, 12793-12798 (2010)
- [7] M. Blodgett, T. Egami, Z. Nussinov, and K. F. Kelton, “Unexpected Universality in the Viscosity of Metallic Liquids”, *Nature Scientific Reports*, **Volume 5**, id. 13837 (2015)
- [8] J. C. Mauro, Y. Yue, A. J. Ellison, P. K. Gupta, and D. C. Allan, “Viscosity of glass-forming liquids”, *PNAS*, **106**, 19780-19784 (2009)
- [9] Z. Nussinov, “A one parameter fit for glassy dynamics as a quantum corollary of the liquid to solid transition”, arXiv: 1510.03875 (2015)
- [10] F. Mallamace, C. Branca, C. Corsaro, N. Leone, J. Spooren, S. Chen, and H. E. Stanley, *PNAS*, **107(52)**: 2245722462 (2010)
- [11] G. E. H. Hentschel, S. Karmakar, I. Procaccia, and J. Zylberg, “Relaxation Mechanisms in Glassy Dynamics: the Arrhenius and Fragile Regimes”, *Phys. Rev. E* **85**, 061501 (2012)
- [12] D. Turnbull, “Under what conditions can a glass be formed?”, *Contemp Phys*, **10**, 473-488 (1969)
- [13] D. Turnbull, “Formation of Crystal Nuclei in Liquid Metals”, *J. Chem. Phys.* **18**, 198 (1950).
- [14] C. A. Angell, “Perspective on the Glass Transition”, *Journ. Phys. and Chem. of Solids*, **49**, 863-871 (1988)